

Study on Properties of Ce(III) doped Co-Mo-P Thin Films Electrodeposited on 45# Steel

Fang Wu^{1,*}, Wei Wang²

¹ College of Artificial Intelligence, Henan Finance University, Zhengzhou 450046, China;

² College of Information Engineering, Zhengzhou University of Technology, Zhengzhou 450044, China;

E-mail: Wu_820edu@126.com

Received: 24 May 2022 / Accepted: 1 July 2022 / Published: 7 August 2022

Ce(III) doped Co-Mo-P thin films were electrodeposited on the surface of 45# steel. The adhesion strength, surface morphology, thickness, crystal phase structure, hardness and magnetic property of the Ce(III) doped Co-Mo-P thin films was studied. The results demonstrate that cerium nitrate concentration has relatively little effect on the adhesion strength, phase composition and preferred orientation of the Ce(III) doped Co-Mo-P thin films, but it will affect the morphology and thickness, which results in different hardness and magnetic properties of Ce(III) doped Co-Mo-P thin films. The surface of the Ce(III) doped Co-Mo-P thin film electrodeposited under the condition of cerium nitrate 60 mg/L is relatively flat, uniform and dense, and has a thickness of about 9.1 μm . The main phases are elemental Co and Co_3Mo , and the (210) crystal plane is preferred orientation. The hardness of the Ce(III) doped Co-Mo-P thin film reaches 532 HV, approximately 1.5 times greater than that of 45# steel substrate, while the maximum coercivity is 931.18 Oe and saturation magnetisation is 101.55 emu/g.

Keywords: Ce(III) doped Co-Mo-P thin films; Cerium nitrate; Electrodeposition; Crystal phase structure; Magnetic property

1. INTRODUCTION

Co-based alloy film or composite film is a type of functional metal film that has good corrosion resistance and excellent magnetic property [1-4]. In addition, it has a good application prospect within the field of micro-electro-mechanical-systems and can be used in micro-computer electrical parts as a means of fulfilling the requirements of high-density storage, decoration and protection. Co-based alloy film or composite film can currently be prepared by electroless plating, vapour deposition, electrodeposition and sputtering [5-10]. Among them, electrodeposition has the advantages of stable

process, convenient operation, and so on. In comparison to other methods, electrodeposition has attracted significant attention in relation to the preparation of Co-based alloy film or composite film.

Co-Mo-P film is a Co-based ternary alloy film, and the introduction of Mo element can control the properties of Co-based films. Rare earth compounds have special properties and they are usually used as additives, which have been confirmed to play a positive role in promoting crystallization nucleation to improve the properties of metal films [11-15]. In order to further improve the properties of Co-Mo-P thin films and broaden their application range, this paper utilises electrodeposition technology to prepare Ce(III) doped Co-Mo-P thin films on the surface of 45# steel from a plating solution that contains cerium nitrate. The adhesion strength, surface morphology, thickness, crystal phase structure, hardness and magnetic property of the Ce(III) doped Co-Mo-P thin films was studied.

2. EXPERIMENTAL

2.1 Chemical agents and pre-treatment of 45# steel

The following chemical agents were used in the experiment: sodium hydroxide, sodium carbonate, hydrochloric acid, sodium chloride, cobalt acetate, sodium molybdate, sodium hypophosphite, sodium citrate, ammonium chloride and cerium nitrate. The purity grade was analytical pure.

A 45# steel sheet was cut using wire cutting and used as the substrate (35 mm×16 mm×1.5 mm), and the pre-treatment process was conducted in the following way: polishing → alkali washing for the removal oil (sodium hydroxide 15 g/L+ sodium carbonate 35 g/L, soaking at 60°C for 10 min) → pickling activation (10% hydrochloric acid, soaking at room temperature for 2 min) → repeated washing with deionised water → cold air drying.

2.2 Electrodeposition of Ce(III) doped Co-Mo-P thin films

The plating solution was prepared according to the standard procedure and the main composition were as follows: cobalt acetate 14 g/L, sodium molybdate 6 g/L, sodium hypophosphite 30 g/L, sodium citrate 72 g/L and ammonium chloride 12 g/L . After stirring evenly, cerium nitrate was added into the plating solution. Different Ce(III) doped Co-Mo-P thin film samples were prepared under the conditions of variation cerium nitrate concentration (20 mg/L, 40 mg/L, 60 mg/L and 80 mg/L). The electrodeposition process conditions were as follows: plating solution temperature (95±0.5)°C, current density 2 A/dm², stirring rate 200 r/min and electrodeposition time 60 min. A Co-Mo-P thin film sample was prepared from the plating solution without cerium nitrate as a comparison, and the main composition of the plating solution and electrodeposition process conditions were the same as above.

2.3 Properties testing and analysis

2.3.1 Adhesion strength of Ce(III) doped Co-Mo-P thin films

According to ASTM D3359-93 standard, the adhesion strength of different Ce(III) doped Co-Mo-P thin films was tested using the grid method. Four transverse and longitudinal crisscrossed cuts were made on the surface of each sample. Press and stick the 3M traceless tape on the cut area, pull off the tape along one side to observe the cuts and evaluate the adhesion strength of different Co-Mo-P thin films according to relevant standards.

2.3.2 Surface morphology, composition and thickness of Ce(III) doped Co-Mo-P thin films

The surface morphology of different Ce(III) doped Co-Mo-P thin films was observed by MERLIN Compact scanning electron microscope, and the composition of different Ce(III) doped Co-Mo-P thin films was observed by X-max80 Electron Energy Disperse Spectroscopy. The surface roughness of different Ce(III) doped Co-Mo-P thin films was measured by SJ-210 roughness meter with 0.25 mm/s scanning rate and 0.8 mm length. Three different positions were selected on the surface of each sample to measure, and the measurement results were averaged to reduce errors. The thickness of different Ce(III) doped Co-Mo-P thin films was measured by a Dektak XT step meter, and each sample was repeated three times to obtain the average of measurement results.

2.3.3 Crystal phase structure of Ce(III) doped Co-Mo-P thin films

D8 Advance X-ray diffractometer and Jade software were combined to analyze the crystal phase structure and preferred orientation of different Ce(III) doped Co-Mo-P thin films. The test voltage was set at 40 kV, the current was set at 40 mA, and the scanning rate was set at 4°/min from 20° to 105°. According to the equation (1), the coefficient of each crystal plane of different Ce(III) doped Co-Mo-P thin films is calculated, and the preferred orientation $TC_{(hkl)}$ is determined.

$$TC_{(hkl)} = \frac{I_{(hkl)}/I_{0(hkl)}}{\sum_{i=1}^n I_{(hkl)}/I_{0(hkl)}} \times 100\% \quad (1)$$

$I_{(hkl)}$ and $I_{0(hkl)}$ represent the diffraction intensity of the Ce(III) doped Co-Mo-P thin film and the standard diffraction intensity of (hkl) crystal plane, respectively.

2.3.4 Hardness and magnetic property of Ce(III) doped Co-Mo-P thin films






The hardness of different Ce(III) doped Co-Mo-P thin films was measured by MV-TEST1000 Vickers hardness tester. A load of 5 N was applied and uniformly unloaded after 15 s. Five points were selected on the surface of each sample, and the measurement results were averaged. The magnetic property of different Ce(III) doped Co-Mo-P thin films was evaluated based on coercivity and saturation magnetization which were tested by Lake-shore8600 Vibrating Sample Magnetometer. The max applied magnetic field was 20000 Gs.

3. RESULTS AND DISCUSSION

3.1 Adhesion strength of Ce(III) doped Co-Mo-P thin films

Table 1 lists the adhesion strength test results of different Ce(III) doped Co-Mo-P thin films. Grades 0~5 indicate a gradual decrease in the degree of adhesion strength between the Ce(III) doped Co-Mo-P thin film and 45# steel substrate. The grade 0 indicates that the Ce(III) doped Co-Mo-P thin film and 45# steel substrate are very closely bonded, and grade 5 indicates that the Ce(III) doped Co-Mo-P thin film is not tightly bonded to 45# steel substrate. It can be seen from Table 1 that cerium nitrate concentration has basically no effect on the adhesion strength of Ce(III) doped Co-Mo-P thin film. The incision area of different Ce(III) doped Co-Mo-P thin films does not appear to fall off, and the incision edge is smooth. The adhesion strength is regarded as an important parameter for metal films [16-18].

Table 1. Adhesion strength test results of different Ce(III) doped Co-Mo-P thin films

Cerium nitrate concentration/ (mg·L ⁻¹)	Grade	Morphology of cut area
0	0	
20	0	
40	0	
60	0	
80	0	

3.2 Surface morphology, composition and thickness of Ce(III) doped Co-Mo-P thin films

Figure 1 shows the surface morphology of 45# steel substrate and different Ce(III) doped Co-Mo-P thin films. It can be seen that Ce(III) doped Co-Mo-P thin films with good uniformity have been successfully electrodeposited on the surface of 45# steel substrate. Some holes and irregularly shaped particles are distributed on the surface of the Co-Mo-P thin films prepared without cerium nitrate. When the cerium nitrate concentration is 20 mg/L, the size of particles on the surface of Ce(III) doped Co-Mo-P thin film decreases, but the compactness is not significantly improved compared with the Ce(III) doped Co-Mo-P thin film prepared without cerium nitrate. This indicates that low cerium nitrate concentration has little effect on the surface morphology of Ce(III) doped Co-Mo-P thin films. With the increase of cerium nitrate concentration to 60 mg/L, the Ce(III) doped Co-Mo-P thin film has few holes and particles, and the surface is uniform and compact.

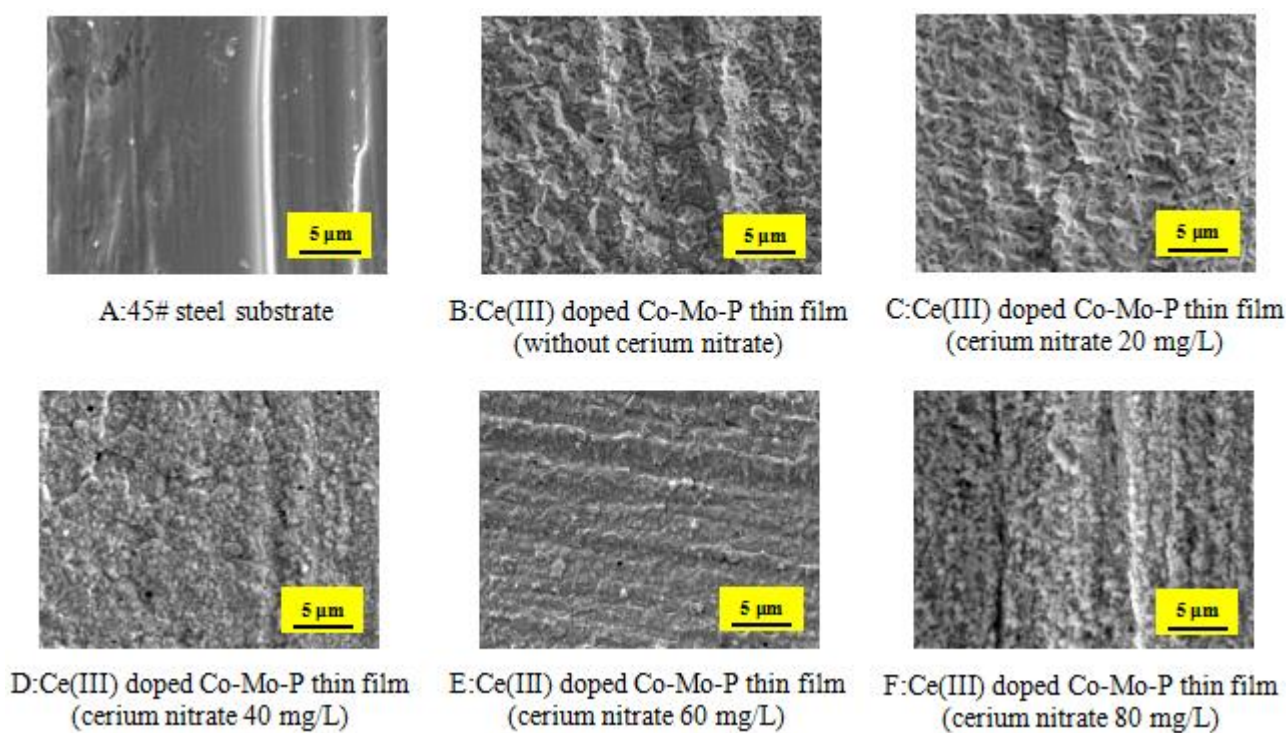


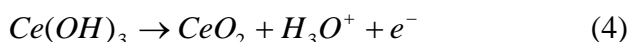
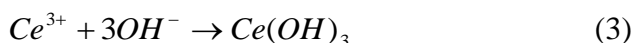
Figure 1. Surface morphology of 45# steel substrate and different Ce(III) doped Co-Mo-P thin films

The complex of cerium nitrate and some components in the plating solution can increase the concentration of free metal ions in the plating solution to accelerate the deposition rate and increase the growth rate of new unit cells which is beneficial to refine the unit cell [19-20]. Therefore, an appropriate increase in the cerium nitrate concentration can improve the compactness of Ce(III) doped Co-Mo-P thin film. In addition, cerium nitrate is easily adsorbed on the surface of 45# steel substrate to form active particles, promote nucleation and increase the distribution density of unit cells. Therefore, appropriate cerium nitrate concentration in the plating solution increases the nucleation rate and refines the unit cell of the Ce(III) doped Co-Mo-P thin film to form compact surface.

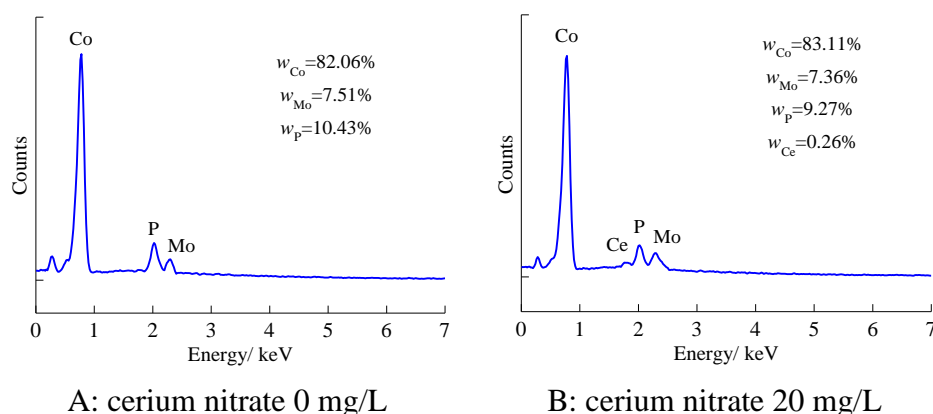
However, when the concentration of cerium nitrate reaches 80 mg/L, the surface of Ce(III) doped Co-Mo-P thin film becomes rough and some large holes will be formed. This is because when the cerium nitrate concentration is too high, the adsorption on the surface of 45# steel substrate reduces the activity of nucleating particles, which leads to a decrease in the distribution density of crystal cells to form the Ce(III) doped Co-Mo-P thin film with roughness surface.

The EDS spectra of different Ce(III) doped Co-Mo-P thin films can be seen in Figure 2. As Figure 2 shows, different Ce(III) doped Co-Mo-P thin films contain Co, Mo, P and Ce element. Although the mass fraction of Ce element is lower than that of Co, Mo and P element, the detection of Ce element in the film confirms that Ce element is involved in the electrodeposition process of Ce(III) doped Co-Mo-P thin films. When the concentration of lanthanum nitrate is 60 mg/L, the mass fraction of Ce element in Ce(III) doped Co-Mo-P thin film is the highest, which is about 1.62%. When the concentration of lanthanum nitrate reaches 80 mg/L, the mass fraction of Ce in Ce(III) doped Co-Mo-P thin film decreases obviously. It has been confirmed that rare earth elements have some special properties, even if rare earth elements enter the film with the deposition process, it can improve the density and properties of the film. Theoretically, the higher the mass fraction of rare earth elements in the film, the more obvious the effect of improving the density and properties of the film. The element distribution of cerium modified Co-based film has reported in various works [21].

The Ce(III) doped Co-Mo-P thin film during electrodeposition is explained by the group of Hamlaoui published in materials chemistry and physics [22-23]. They verify that the CeO_2 and $Ce(OH)_3$ can be found in the Ce(III) doped Co-Mo-P thin film. The mechanism is listed below.



During the electrodeposition process, the concentration of OH^- near the cathode increases due to hydrogen precipitation. Moreover, nitrate is reduced to further increase the concentration of OH^- near the cathode. The OH^- can combine with Ce^{3+} to form cerium $Ce(OH)_3$. Some of the cerium hydroxide can change to cerium oxide. Therefore, the element of Ce can be found in the EDS spectra which are similar to the result we find.



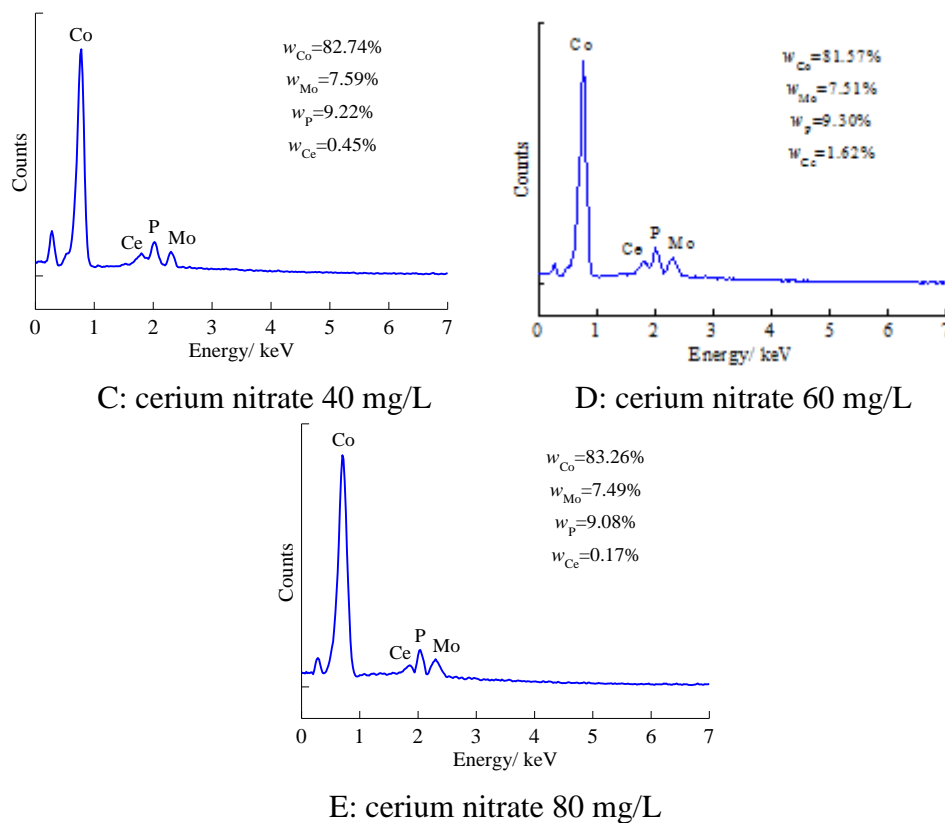


Figure 2. EDS spectra of different Ce(III) doped Co-Mo-P thin films

Figure 3 shows the thickness of different Ce(III) doped Co-Mo-P thin films. It can be seen from Figure 3 that the thickness of Ce(III) doped Co-Mo-P thin film is not affected with or without cerium nitrate. However, when cerium nitrate concentration is too high, the thickness of Ce(III) doped Co-Mo-P thin film decreases obviously to less than 7 μm . It is concluded that the adsorption of cerium nitrate on the surface of 45# steel substrate inhibits the nucleation process to a certain extent, resulting in the decrease of nucleation rate and formation rate of Ce(III) doped Co-Mo-P thin film resulting in the decrease of thickness, which will have an adverse effect on the properties of Ce(III) doped Co-Mo-P thin film.

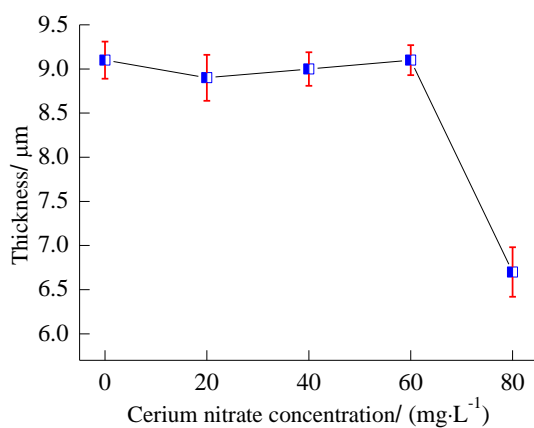


Figure 3. Thickness of different Ce(III) doped Co-Mo-P thin films

3.3 Crystal phase structure of Ce(III) doped Co-Mo-P thin films

Figure 4 shows the XRD patterns of different Ce(III) doped Co-Mo-P thin films. According to XRD analysis, different Ce(III) doped Co-Mo-P thin films all have crystalline structure, and the main phases are elemental Co and Co_3Mo . Among them, Co_3Mo phase is formed due to Mo solid solution in the lattice gap of Co, which has been confirmed by relevant studies [24]. The formation of Co_3Mo phase may cause lattice distortion, which is beneficial to improve the properties of Ce(III) doped Co-Mo-P thin films.

Through a comparison of the XRD patterns of different Ce(III) doped Co-Mo-P thin films, it is found that the two diffraction peaks of the elemental Co phase correspond to angles of approximately 45° and 83° , and the crystal plane is (210) and (411). The diffraction peaks of the Co_3Mo phase correspond to an angle of 65° and crystal plane of (022) respectively. The results show that cerium nitrate concentration has no effect on the phase composition and diffraction peak position of Ce(III) doped Co-Mo-P thin films. However, as the cerium nitrate concentration increases to 60 mg/L, the diffraction peak intensity of Co_3Mo phase is obviously enhanced, which indicates that crystallinity of the phase becomes better, which can also reflect the refinement of the crystal cell.

The coefficients of each crystal plane of different Ce(III) doped Co-Mo-P thin films are calculated shown in Figure 5. As can be seen from Figure 4, the coefficient of (210) crystal plane is the largest, followed by the coefficient of (022) crystal plane, and the coefficient of (411) crystal plane is the smallest. Some studies show that the larger the texture coefficient is, the corresponding crystal face presents a preferred orientation [25-26]. Therefore, different Ce(III) doped Co-Mo-P thin films have preferred orientation of (210) crystal plane.

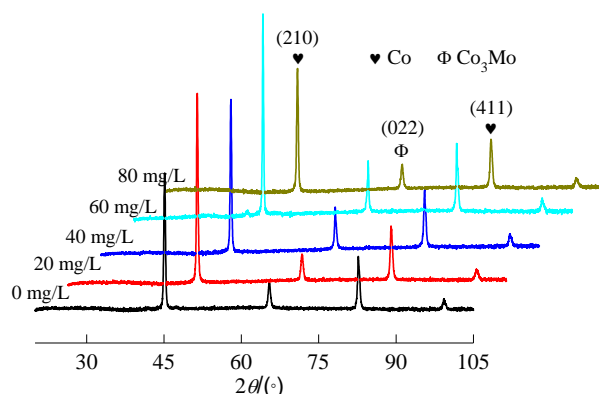


Figure 4. XRD patterns of different Ce(III) doped Co-Mo-P thin films

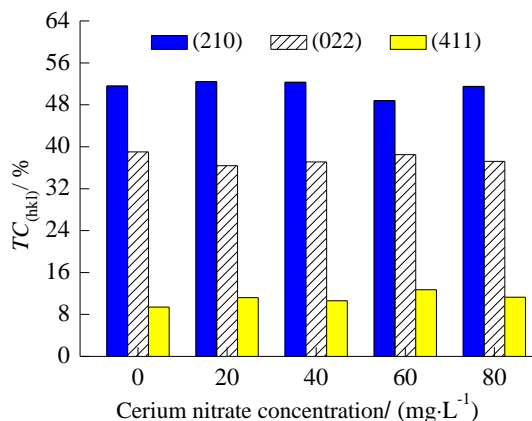


Figure 5. Texture coefficient of each crystal plane of different Ce(III) doped Co-Mo-P thin films

3.4. Hardness and magnetic property of Ce(III) doped Co-Mo-P thin films

Figure 6 shows the hardness of different Ce(III) doped Co-Mo-P thin films. As can be seen from Figure 6, the hardness of the Ce(III) doped Co-Mo-P thin films prepared without cerium nitrate is 468 HV, which is at least two times larger than that of 45# steel substrate (210 HV). With the increase of cerium nitrate concentration to 60 mg/L, the hardness of the Ce(III) doped Co-Mo-P thin film gradually increases to 532 HV. On the one hand, the surface of Ce(III) doped Co-Mo-P thin film tends to be smooth by appropriate increase of cerium nitrate concentration resulting in the improvement of the densification enhancement of resistance to local plastic deformation. On the other hand, appropriately increasing cerium nitrate concentration can improve the crystallinity of Co₃Mo phase, which is also conducive to the refinement and densification of Ce(III) doped Co-Mo-P thin film cells, thus improving the bearing capacity and resistance to local plastic deformation. However, when cerium nitrate concentration is too high, the surface smoothness, compactness and thickness of Ce(III) doped Co-Mo-P thin film decrease to reduce the resistance to local plastic deformation and hardness.

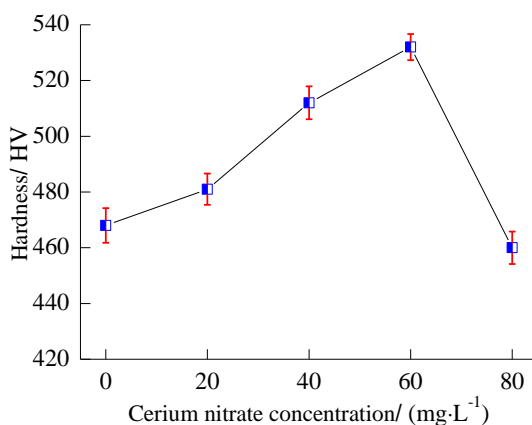


Figure 6. Hardness of 45# steel substrate and different Ce(III) doped Co-Mo-P thin films

Figure 7 and Figure 8 show the magnetic property of different Ce(III) doped Co-Mo-P thin films. It can be seen that the Ce(III) doped Co-Mo-P thin films prepared from the plating solution

containing different cerium nitrate concentration has different magnetic property. With the increase of cerium nitrate concentration, the coercivity and saturation magnetization of Ce(III) doped Co-Mo-P thin films both increase gradually and then decline dramatically. According to the previous analysis, appropriate increase of cerium nitrate concentration is beneficial to increase the nucleation rate and refine the unit cell of the Ce(III) doped Co-Mo-P thin film which contributes to the increase of coercivity and saturation magnetization. However, when cerium nitrate concentration reaches 80 mg/L, the surface of the Ce(III) doped Co-Mo-P thin film becomes rough and some large holes are formed resulting in the decrease of magnetic property. The Ce(III) doped Co-Mo-P thin film electrodeposited under the condition of cerium nitrate 60 mg/L has the best magnetic property, the maximum coercivity and saturation magnetization is 931.18 Oe and 101.55 emu/g respectively.

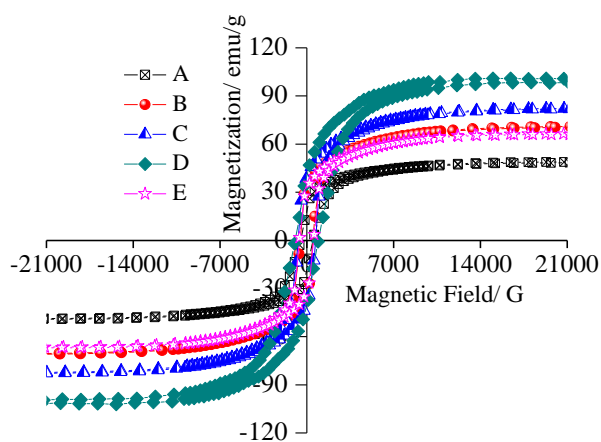


Figure 7. Magnetic property of different Ce(III) doped Co-Mo-P thin films; A-cerium nitrate 0 mg/L; B-cerium nitrate 20 mg/L; C-cerium nitrate 40 mg/L; D-cerium nitrate 60 mg/L; E-cerium nitrate 80 mg/L

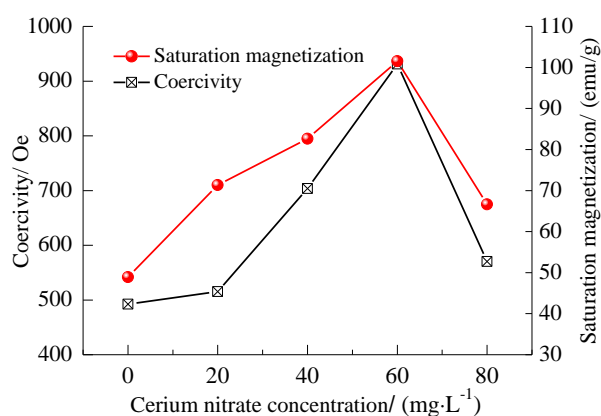


Figure 8. Coercivity and saturation magnetization of different Ce(III) doped Co-Mo-P thin films

4. CONCLUSIONS

(1) Adhesion strength, surface morphology, thickness, crystal phase structure, hardness and magnetic property of Ce(III) doped Co-Mo-P thin films is studied. An appropriate increase in the

cerium nitrate concentration is beneficial for refining the unit cell, improving the compactness, and enhancing the hardness and magnetic property of Ce(III) doped Co-Mo-P thin film. However, the high cerium nitrate concentration leads to the deterioration of surface compactness of the Ce(III) doped Co-Mo-P thin film, the decrease of hardness and the decline of magnetic property.

(2) When the cerium nitrate concentration is 60 mg/L, the Ce(III) doped Co-Mo-P thin film has the smallest crystal cells, smooth and uniform surface, with a thickness of 9.1 μm and a preferred orientation of (210) crystal plane. The hardness of the Ce(III) doped Co-Mo-P thin film is 532 HV, which is 1.5 times greater than the hardness of the 45# steel substrate. The coercivity and saturation magnetization of the Ce(III) doped Co-Mo-P thin film are up to 931.18 Oe and 101.55 emu/g respectively, showing the best magnetic property.

References

1. C. W. Qiang, J. C. Xu, S. T. Xiao, Y. J. Jiao, Z. Q. Zhang, Y. Liu, L. L. Tian and Z. G. Zhou, *Appl. Surf. Sci.*, 257 (2010) 1371.
2. Y. Pei, Y. Yang, F. F. Zhang, P. Dong, R. Baines, Y. C. Ge, H. Chu, P. M. Ajayan, J. F. Shen and M. X. Ye, *ACS Appl. Mater. Interfaces*, 9 (2017) 31887.
3. N. Fukumuro, J. Nishiyama, K. Shigeta, Y. Morimoto, H. Takagami, S. Yae and H. Matsuda, *Electrochem. Commun.*, 9 (2007) 1185.
4. J. X. Xu and Y. Xu, *Mater. Lett.*, 60 (2006) 2069.
5. N. Fukumuro, J. Nishiyama, S. Yae and H. Matsuda, *Trans. Mater. Res. Soc. Jpn.*, 35 (2010) 55.
6. Y. G. Kim, D. J. Byun, C. Hutchings and P. A. Dowben, *J. Appl. Phys.*, 70 (1991) 6062.
7. M. S. Safavi, M. Fathi, V. Charkhesht, M. Jafarpour and I. Ahadzadeh, *Metall. Mater. Trans. A*, 51 (2020) 6740.
8. R. Suresh, P. Sathishkumar, S. Kumaravelan and S. Seshadri, *Surf. Rev. Lett.*, 28 (2021) 2050039.
9. A. Q. Zhang, Y. H. Xiao, Y. Cao, H. Fang, Y. Zhang, P. Das and H. Zhang, *J. Solid State Electrochem.*, 25 (2021) 1503.
10. X. M. Cai, X. Q. Su, F. Ye, H. Wang, X. Q. Tian, D. P. Zhang, P. Fan, J. T. Luo, Z. H. Zheng, G. X. Liang and V. A. Roy, *Appl. Phys. Lett.*, 107 (2015) 083901.
11. Y. Gao, J. H. Wang, J. Yuan and H. Q. Li, *Appl. Surf. Sci.*, 364 (2016) 740.
12. J. C. Kuang and Y. Huang, *J. Rare Earths*, 28 (2010) 469.
13. J. Sun and X. W. Zhang, *Anti-Corros. Methods Mater.*, 60 (2013) 194.
14. H. Ashassi-Sorkhabi, M. Moradi-Haghighi and M. G. Hosseini, *Surf. Coat. Technol.*, 202 (2018) 1615.
15. J. Yuan, J. H. Wang, Y. Gao, J. Miao and W. B. Hu, *Thin Solid Films*, 632 (2017) 1.
16. N. Akcay, M. Tivanov and S. Ozcelik, *J. Electron. Mater.*, 50 (2021) 1452.
17. C. H. Zhang, C. Li, X. Q. Si, Z. J. He, J. L. Qi, J. C. Feng and J. Cao, *Appl. Surf. Sci.*, 529 (2020) 147113.
18. P. J. Zhang, X. R. Zou, S. L. Zhang, C. Q. Xia, C. Y. Liang, N. Liu and H. S. Wang, *J. Mater. Sci.*, 56 (2021) 13313.
19. K. Aramaki, *Corros. Sci.*, 46 (2004) 1565.
20. Y. D. Yu, G. Y. Wei, L. Jiang and H. L. Ge, *Int. J. Electrochem. Sci.*, 15 (2020) 1108.
21. J. Wang, A. Yoshida, P. Wang, T. Yu, Z. D. Wang, X. G. Hao, A. Abudula and G. Q. Guan, *Appl. Catal., B*, 271 (2020) 118941.
22. Y. Hamlaoui, F. Pedraza, C. Remazeilles, S. Cohendoz, C. Rebere, L. Tifouti and J. Creus, *Mater. Chem. Phys.*, 113 (2009) 650.

23. Y. Hamlaoui, L. Tifouti, C. Remazweilles and F. Pedraza, *Mater. Chem. Phys.*, 120 (2010) 172.
24. C. H. Lee, K. L. Yu, M. H. Lee, J. C. A. Huang and G. P. Felcher, *J. Magn. Magn. Mater.*, 209 (2000) 110.
25. B. Benhaoua, A. Rahal and S. Benramache, *Superlattices Microstruct.*, 68 (2014) 38.
26. A. Pandey, S. Dalal, S. Dutta and A. Dixit, *J. Mater. Sci.: Mater. Electron.*, 32 (2021) 1341.

© 2022 The Authors. Published by ESG (www.electrochemsci.org). This article is an open access article distributed under the terms and conditions of the Creative Commons Attribution license (<http://creativecommons.org/licenses/by/4.0/>).